REPORT DOCUMENTATION PAGE	*Form Approved* *OMB No. 0704-0188*

1. REPORT DATE *(DD-MM-YYYY)*	**2. REPORT TYPE**	**3. DATES COVERED** *(From - To)*
10/08/2007	Final	01/01/05-31/12/06

4. TITLE AND SUBTITLE
High-Fidelity Real Gas Model for RF Excited Plasma Flow Contraol

5a. CONTRACT NUMBER

5b. GRANT NUMBER
FA9550-05-1-0074

5c. PROGRAM ELEMENT NUMBER

6. AUTHOR(S)
Roy, Dr. Subrata

5d. PROJECT NUMBER

5e. TASK NUMBER

5f. WORK UNIT NUMBER

7. PERFORMING ORGANIZATION NAME(S) AND ADDRESS(ES)
Kettering University
1700 W. Third Avenue
Flint, MI 48504

8. PERFORMING ORGANIZATION REPORT NUMBER
530140

9. SPONSORING/MONITORING AGENCY NAME(S) AND ADDRESS(ES)
AFOSR
875 North Randolph Street
Arlington, VA 22308
Dr John Schmisseur/NA

10. SPONSOR/MONITOR'S ACRONYM(S)
AFOSR/PKC

11. SPONSOR/MONITOR'S REPORT NUMBER(S)

12. DISTRIBUTION/AVAILABILITY STATEMENT
Approved for public release, distribution unlimited

AFRL-SR-AR-TR-07-0504

13. SUPPLEMENTARY NOTES

14. ABSTRACT
We demonstrate the prediction capability a self consistent finite-element formulation for mitigating inert gas flow separation using rf-driven dielectric barrier discharge. Specifically, several physical and geometric parameters such as the amplitude and shape of excitation, dielectric constants, initial ionization level, and electrode shape are studied. The effect of polyphase power supply to an array of actuators has also been explored. It is found that (a) favorable ranges of frequency and electric field exist for most effective flow control, (b) the momentum transfer to the neighboring gas is cumulative for an optimum phase angle and distance between the exposed electrodes. Also streamwise momentum transfer does not keep on increasing with the number of actuators. We extend our work towards developing a multidimensional first principles theoretical model of the non-equilibrium real gas discharge. The electric force field generated by asymmetrically arranged plasma actuator We have worked in close collaboration with Dr. Datta Gaitonde (VAAC/AFRL) code and to simulate electrodynamic mitigation of three-dimensional wing stall about a symmetric airfoil. These efforts set the basis for active flow control over a vehicle forebody.

15. SUBJECT TERMS
Plasma Actuators, Flow Control, Dielectric Barrier Discharge, Finite Elements, Self-consistent Formulation

16. SECURITY CLASSIFICATION OF:			**17. LIMITATION OF ABSTRACT**	**18. NUMBER OF PAGES**	**19a. NAME OF RESPONSIBLE PERSON**
a. REPORT	**b. ABSTRACT**	**c. THIS PAGE**			Ms. Arlene Hunt
					19b. TELEPHONE NUMBER *(Include area code)* 810-762-9934

FINAL REPORT FOR AFOSR GRANT NUMBER FA9550-05-1-0074

PROJECT TITLE: HIGH-FIDELITY REAL GAS MODEL FOR RF EXCITED PLASMA FLOW CONTROL

Principal Investigator: Subrata Roy
Kettering University
Department of Mechanical Engineering
1700 West Third Avenue
Flint, MI 48504

Abstract

This report is a summary of a two-year effort by the PI's research team and collaborators. We have demonstrated the prediction capability of module-based multiscale ionized gas (MIG) flow finite-element code for mitigating inert gas flow separation using rf-driven dielectric barrier discharge. We extended our work towards developing a multidimensional first principles theoretical model of the non-equilibrium real gas discharge. The electric force field generated by asymmetrically arranged plasma actuators operating at rf is self-consistently coupled to the gas dynamics of the air-like N_2/O_2 gas mixtures. Specifically, several physical and geometric parameters such as the amplitude and shape of excitation, dielectric constants, initial ionization level, and electrode shape are studied. The effect of polyphase power supply to an array of actuators has also been explored. It is found that (a) favorable ranges of frequency and electric field exist for most effective flow control, (b) the momentum transfer to the neighboring gas is cumulative for an optimum phase angle and distance between the exposed electrodes. Also, streamwise momentum transfer does not keep on increasing with the number of actuators. We have worked in close collaboration with Dr. Datta Gaitonde (VAAC/AFRL) to integrate MIG with FDL3DI code and to simulate electrodynamic mitigation of three-dimensional wing stall about a symmetric airfoil. Similar collaboration with VAAC/AFRL researchers is underway towards modeling plasma control of transitional vortical flow over a low sweep delta wing. These efforts set the basis for applying the simulation method for actively controlling vortical flows past common aerodynamic configurations like a vehicle forebody.

I. Introduction

Recent successful experiments and simplified numerical models for boundary layer flow actuation using dielectric surface discharge at atmospheric pressures show tremendous potential for aerospace and many other applications [1-6]. These watt-level actuators can efficiently apply large electrohydrodynamic (EHD) forces in a relatively precise and self-limiting manner, have rapid switch-on/off capabilities and require no moving parts. A detailed theoretical understanding of the actuation mechanism is necessary to design these devices for more effective momentum injection for better flow control. Typical electrode arrangements for these actuators have a grounded electrode which is surrounded by an insulator and a voltage fluctuating with radio frequency (rf) is applied to the electrode exposed to the gas. The experimental data suggest 1-20 kV peak-to-peak applied voltage with 2-50 kHz rf is suitable for these actuators operating at atmospheric pressure. The plasma discharge at this pressure is highly collisional causing an efficient energy exchange between charged and neutral species. Numerical simulation predicted new insight into the near wall momentum exchange physics. It is observed that dielectric surface becomes negatively charged for most of the power cycle and a time averaged force acts on the plasma predominantly downstream, with a transverse component towards the wall. Momentum of the plasma couples to real gas through collisions, which enhances near-wall momentum yielding a wall-jet-like feature for quiescent gas. A suitable range for electrical and physical control parameters has also been identified for which, the induced momentum most effectively mitigates separated flow over a flat plate and the wing stall characteristics. It is found that the momentum transfer to the neighboring gas is cumulative for an array of actuators showing, however, a diminishing return with increasing number of electrodes.

II. Objective

This numerical simulation effort aims to explore the transient plasma-gas interaction processes of a near electrode RF excited dielectric barrier (optical glow) discharge for helium gas and air-like N_2/O_2 mixture at atmospheric conditions. These processes have been shown experimentally to have profound impact on both high- and low-speed flows relevant to the Air Force interest. The research goal is to develop from first principles a self-consistent theoretical model of suitable complexity, to implement it into a powerful, robust and efficient numerical tool, and finally to demonstrate the effect of surface plasma discharge on real gas flow about a realistic geometry. Comprehensive understanding of the pertinent mechanisms will significantly impact the high speed flight endeavor; enable introduction of new concepts exploiting fundamental EHD flow control and guide current and future experimental efforts.

III. Approach

Due to a combination of electrodynamic and collisional processes the proper mechanism of which is yet to be theoretically resolved, charge separated particles induce the gas particles to move. For accuracy and fidelity, it is essential that the force relations be derived from first principles through a simulation of the elementary mechanisms that yield the discharge. We are developing [4-9] such models in the following manner. First, a drift diffusion partially ionized gas model for atmospheric air-like N_2/O_2 gas mixture is formulated for nine species. Various reaction rate coefficients [10] are obtained based on electron temperature calculated from the instantaneous electric field. The reactions include momentum transfer, molecular ionization, dissociation, dissociative recombination and secondary electron emission. Atmospheric ratio of 3.6 is taken for nitrogen to oxygen gas molecules. The model is anchored in the module based multiscale ionized gas (MIG) flow code [4-6, 11-13]. The self-consistent formulation is solved using a Galerkin variational formulation based finite-element method [12,13] to obtain electron, positive and negative ions and neutral species densities of nitrogen and oxygen, and the electric potential in two spatial dimensions.

The EHD body force thus calculated from separated space charge and electric field is then employed for solving gas hydrodynamic equations. Barrier discharges in air-like N_2/O_2 mixtures consist of a multitude of micro and nanoscale discharges [8]. MIG implements a powerful high-fidelity finite-element (FE) procedure adapted from fluid dynamics to overcome the stiffness of the equations generated by multi-species charge separation phenomena. Implemented FE techniques are especially suitable for operating at disparate spatial and temporal scales and for their adaptability to arbitrary multidimensional geometries and boundary conditions [13]. Here, a 2D biquadratic basis polynomial is employed to interpolate the state variables along with implicit time marching to solve the continuity and momentum equations for all species and gas. The solution process consists of two steps – first solve for all species (including neutrals) to calculate the charge separation and electric field up to a periodic asymptote with a timestep of up to 100 times the dielectric relaxation timescale, then use those as body force to predict the air velocity and continuity evolving in time with the flow timescale. The solution of the Newton iteration for the resulting matrices is convergent at any given time step when the maximum value of the residual relative L_2 norm for each of the state variable becomes smaller than a convergence criterion.

Several cases including various electrode configurations and polyphase power input are simulated using both helium and air as working gas. The solutions computed are then qualitatively benchmarked with the reported test data. The computed EHD force data are also transitioned to the VAAC/AFRL researchers who predicted the flow control mechanism over a stalled NACA 0015 wing.

IV. Discharge Formulation

The following two-dimensional three species collisional plasma-sheath model is solved.

Charge continuity: $$\frac{\partial n_\alpha}{\partial t} + \frac{\partial n_\alpha V_{\alpha j}}{\partial x_j} = n_e z - r n_e n_i \tag{1a}$$

Charge momentum: $$n_\alpha V_{\alpha j} = -\mathrm{sgn}(e) n_\alpha \mu_\alpha \frac{\partial \phi}{\partial x_j} - D_\alpha \frac{\partial n_\alpha}{\partial x_j} \tag{1b}$$

Potential: $$\varepsilon \left(\frac{\partial^2 \phi}{\partial x_j^2} \right) = e(n_e - n_i) \tag{2}$$

Neutral continuity: $$\frac{\partial n_n}{\partial t} + \frac{\partial n_n V_{nj}}{\partial x_j} = -n_e z + r n_e n_i \tag{3}$$

The charge particle $\alpha = e,i$ distributions are considered non-Maxwellian and inertia terms are neglected. The electron temperature is nearly uniform at 1eV = 11,600K and the ions and neutrals are in thermal equilibrium at 300K. The working gas, helium, is maintained at bulk pressure p = 300 torr and temperature T = 300K.

Transport properties are taken from the literature. The electron diffusion is obtained from Einstein relation, $D_e = (T_e / e)\mu_e$, where T_e is the energy in electron volts, e is the elementary charge, ε is the permittivity, and $\mu_e = e/(m_e \nu_{eh})$ is mobility of an electron, where $\nu_{en} \approx 10^{12}$/s is the electron-neutral collision frequency. We emphasize that transport properties used from the published literature are to be taken as nominal values facilitating the development of the numerical framework, rather than providing new thermo-chemical data for these discharges. Similarly, the ion diffusion D_i=500 cm^2/s at 300K, and the ion mobility μ_i is given as:

$$\begin{aligned} p\mu_i &= 8\times 10^3 \left(1 - 8\times 10^{-3} E/p\right) \text{ cm}^2\text{V}^{-1}\text{s}^{-1}\text{torr}, \text{ for } E/p \le 25 \text{ V cm}^{-1}\text{torr}^{-1} \\ p\mu_i &= \frac{4.1\times 10^4}{\sqrt{E/p}} \left(1 - \frac{27.44}{(E/p)^{3/2}}\right) \text{ cm}^2\text{V}^{-1}\text{s}^{-1}\text{torr}, \text{ for } E/p > 25 \text{ V cm}^{-1}\text{torr}^{-1} \end{aligned} \tag{4}$$

where $E=\sqrt{E_x^2+E_y^2}$ is the electric field magnitude with components $E_j=-\partial\phi/\partial x_j$ and p is the gas pressure. The index j takes the values x and y. The ionization rate z for helium gas used here is:

$$z=\mathrm{A}\exp\left(\frac{-\mathrm{B}}{(E/p)^{0.4}}\right)p\mu_e E\ \mathrm{s}^{-1};\quad \mathrm{A}=4.4\ \mathrm{cm}^{-1}\mathrm{torr}^{-1}\ \text{and}\ \mathrm{B}=14\ [\mathrm{V/(cm\ torr)}]^{0.4} \tag{5}$$

where, n_e is the electron number density. The coefficient of recombination on the right hand side of Eqn. (1a) and (3) is given as, $r=\langle V_{\mathrm{eth}}\sigma_{ei}^{r}(V_{\mathrm{eth}})\rangle=1.09\times10^{-20}T^{-9/2}n_e\,\mathrm{m^3/s}$. Here, V_{eth} is the electron thermal velocity and σ_{ei} is the electron-ion collision cross-section. For simplicity, we have presently ignored recombination effect on momentum, as well as secondary emission, at this stage.

The dynamics of neutral particles are determined using the following neutral momentum equations:

$$\frac{\partial V_{nj}}{\partial t}+V_{nl}\frac{\partial V_{nj}}{\partial x_l}=\frac{\varpi}{m_n n_n}\frac{\partial}{\partial x_j}\left[\varepsilon\left(\frac{\partial\phi}{\partial x_l}\right)^2\right]+\frac{m_e n_e}{m_n n_n}\nu_{en}\left(V_{ej}-V_{nj}\right)+\frac{Mn_i}{m_n n_n}\nu_{in}\left(V_{ij}-V_{nj}\right)+n_e zV_{ij}/n_n \tag{6}$$

The averaged velocity of the fluid of density $\rho\approx m_n(n_n+n_i)$ is based on the following momentum equation:

$$\frac{\partial V_{fi}}{\partial t}+V_{fl}\frac{\partial V_{fi}}{\partial x_l}=\frac{\varpi}{\rho}e(n_i-n_e)E_i-\frac{\mathrm{R}T}{\rho}\frac{\partial\rho}{\partial x_j}+\frac{\partial}{\partial x_l}\tau_{jl}, \tag{7}$$

where $\tau_{jl}=\frac{\mu}{\rho}\left(\frac{\partial V_{fl}}{\partial x_j}+\frac{\partial V_{fj}}{\partial x_l}\right)-\frac{2}{3}\frac{\mu}{\rho}\frac{\partial V_{fk}}{\partial x_k}\delta_{jl}$ with μ as the gas viscosity ($=2.066\times10^{-5}$ Ns/m^2) and δ_{jl} is the Kronecker delta. The factor ϖ introduced to modulate the effect of electric field is set to unity.

The multiscale ionized gas (MIG) flow code was used to solve Eqns. (1)-(7). MIG implements a versatile high-fidelity finite-element (FE) procedure adapted from fluid dynamics to overcome the stiffness of the equations generated by multi-species charge separation phenomena. FE techniques are especially suitable for their adaptability to arbitrary multidimensional geometries and boundary conditions. Here, a 2D bilinear finite element formulation is employed together with 4th order Runge-Kutta time marching to solve the continuity and momentum equations for all species and fluid. The solution process consists of two steps. First, using Eqns. (1a), (2), (3) and (6), a global matrix is formed and solved simultaneously obviating the need for any special sub-iteration for the Poisson solver. The species density and charge velocity thus calculated are then used in Eqn. (7) to predict the fluid velocity. The Galerkin weak statement associated with a variational integral underlines the development of this numerical algorithm. The solution of the Newton iteration is converged at any given timestep when the maximum value of the residual, relative norm for each of the state variables, becomes smaller than a chosen convergence criterion of 10^{-4}.

The computational domain (x,y: 0,0.01m) consists of a lower half (y:0,0.005m) insulator with dielectric constant $\varepsilon_d = 4.5\ \varepsilon_0$, and a upper half filled with inert helium gas of $\varepsilon_f = 1.0055\ \varepsilon_0$ where ε_0 is permittivity of vacuum. Inside the insulator the current due to motion of charged particles is forced to zero while the displacement current is balanced with the total current at the gas-dielectric boundary. The schematic in Figure 1 shows two electrodes in which the bottom electrode is grounded, $\varphi(0)= 0$, and a sinusoidal RF alternating potential $\varphi_{rf} = \varphi_{rms}\sin 2\pi ft$ with $\varphi_{rms}=1$ kV and f=5 kHz is applied to the top electrode. Each electrode is infinitesimally thin and 2mm long.

In order to identify the effect of geometric configuration two different electrode arrangements were simulated. In the first, the two electrodes were kept vertically aligned. Hereafter, we will denote this as the symmetric configuration. In the second case, the electrodes are offset horizontally by 2mm. This will be noted as the asymmetric configuration. A decrease in the offset horizontally and/or vertically increases the electric field for the same applied rms potential which in effect increases induced electric force. For all simulations electrons are assumed to be isothermal at the boundary and maintained at 1eV (~11,600K) while the ions are cold (300K) at 300 torr. The electron flux at the exposed electrode is based on the electron thermal velocity and is directed towards the wall. Homogeneous Neumann boundary condition ($\partial n_i/\partial x=0$) is imposed for ions at the exposed electrode. The solutions are verified by qualitative comparison with published results. The simulations are then employed to explore the enhancement of near wall fluid velocity.

The ionized helium gas is numerically modeled using the finite-element based MIG flow code. The code is modular and separate subroutines can be written to model different physics. Here, the equation sets (1) – (6) can be written with operator L as L ($\mathbf{q}$) = 0 where $\mathbf{q}$ contains state variables like number densities, velocities and potential. Multiplying with a permissible test function η and integrating over the spatially discretized domain Ω, the variational statement results in the weak form

$$WS^h = \Im_e\left(\int_{\Omega_e}[\eta L(q)d\tau]\right)_e = 0$$

for a discretization h of $\Omega = \cup\Omega_e$ and $\Im_e$ is the non-overlapping sum over the elements. Thus, for example, the GWS form of Eq. (2) becomes,

$$\sum_e\left(\int_{\Omega_e}\frac{d\eta}{dz}\frac{d\eta^T}{dz}dz\{\phi\}_e + \int_{\Omega_e}\eta\eta^T dz\{n_e\}_e - \int_{\Omega_e}\eta\eta^T dz\{n_i\}_e - \int_{\Omega_e\cap\partial\Omega_e}\eta\frac{d\eta^T}{dz}dz\{\phi\}_e = F_\phi\right)_e \tag{8}$$

where F_ϕ is the solution residual.

The Jacobian matrix $J=[\partial F/\partial \mathbf{q}]$ in the global $[J].\{\partial q\} = -\{F\}$ is resolved using LU-decomposition scheme for updating change in discretized solution vector $\mathbf{q}$ at each iteration. The terminal non-linear ordinary differential equation (ODE) systems are solved using implicit Euler method for temporal evolution and N-R iterative algorithm for the non-linear matrix algebra. The convergence criterion for all variables at any iteration is set at 10^{-4}. Solution stability is ensured by appropriate selection of time marching step size and the introduction of artificial diffusion.

V. Major Developments

1. Helium discharge model for quiescent flow

For 6 kHz and 1.6 kV peak-to-peak with alumina insulator, model predictions for charge densities, the electric field and gas velocity distributions are shown to mimic trends reported in the experimental literature. We also predict the electron charge accumulation on the dielectric surface (Figure 1a,b) self-limiting the discharge and influencing the essentially unidirectional charge-neutral momentum exchange forming a wall jet (Figure 1c). The velocity field based on a quiescent flow initial condition shows streamwise component of the computed gas velocity in Figure 1c and depicts a strong wall jet downstream of the rf electrode away from the dielectric surface. The highest momentum transfer between the gas and the charge particles occur slightly downstream of the peak force location shown in Figure 1d. The local vertical line plots at six streamwise locations describe how the flow velocity increases responding to the increase in axial electric field and experimental results show very similar feature [1]. The peak jet velocity is ~1.7 times the calculated freestream velocity.

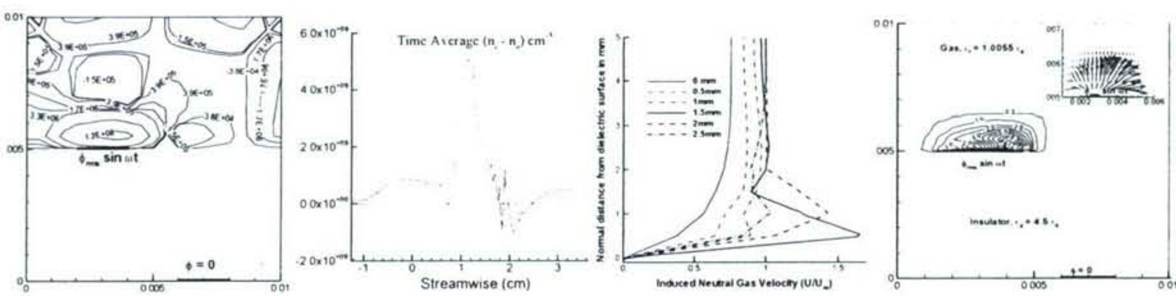

(a) (b) (c) (d)

Figure 1: Plasma actuation of quiescent helium gas. (a) Charge particle distribution shows electron accumulation on the dielectric, (b) time average of charge density, (c) streamwise gas velocity profiles at different locations along the flow, (d) force variation at the peak of the cycle.

2. Helium discharge model for separated flow

Higher-fidelity models are included to yield a more sophisticated framework to predict discharge-induced momentum exchange. Here, the complete problem of a dielectric barrier discharge based separation control with axially displaced electrodes is simulated in a self-consistent manner. The body force is computed self-consistently from the three-body electro gas dynamics using the applied rf potential and the dielectric properties of insulator and gas media based on first principles. For 5 kHz and 1 kV with Kapton dielectric, specific details of the computed flow components and streamwise force is given in Figures 2a-2c. While the normal force component is primarily downward, the time average of the streamwise force component in Figure 2d shows the dominance of the positive force to push the fluid in the forward direction. Line traces show the direction of force which will guide the local flow. Figure 2e shows the eradication process of the separation bubble formed due to the flow pas t a flat plate maintained at +12 deg AOA. More investigation is needed to ascertain optimum electrochemical parameters.

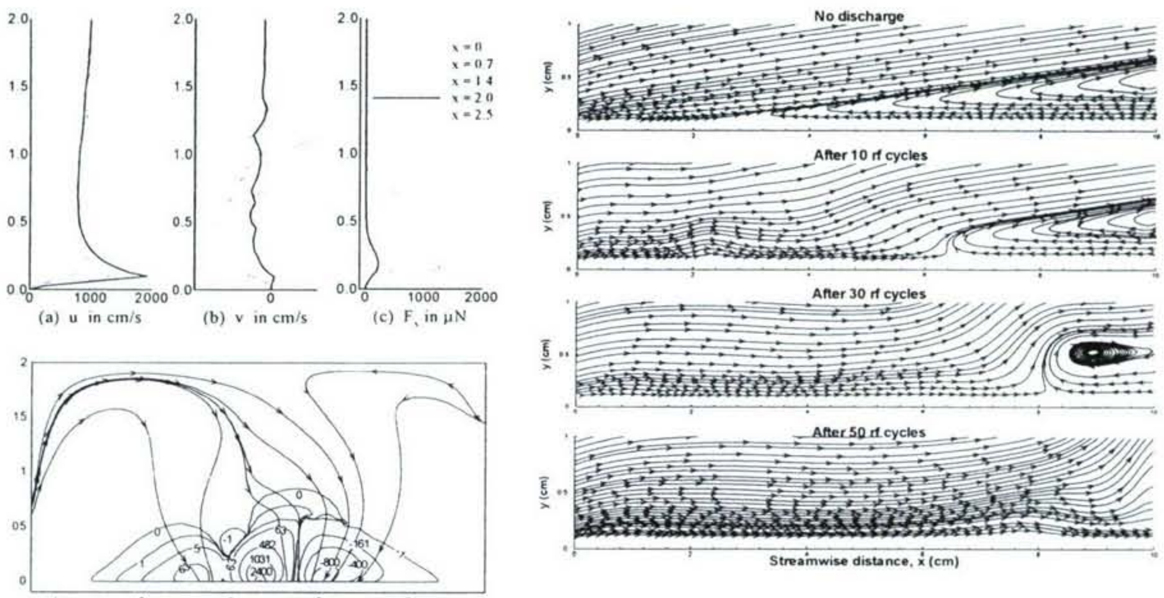

(e) Time evolution of separation control, near wall view

(d) Time averaged volume specific force field

Figure 2: (a-c) Force and velocity details, (d) Time average of streamwise force about the surface of the actuator shows the dominance of the forward (positive) component, (e) Separation control.

3. Polyphase, multiple electrodes and other control parameters:

For 1 mm thick Kapton polyimide dielectric and 12 mm long electrodes, some effective control parameters for active separation mitigation using asymmetric dielectric barrier discharges is studied by considering the weakly ionized helium gas flow past a flat plate at an angle of attack of 12 deg. Figures 3a-f plot the summary results after 50 rf cycles. It is observed that the time averaged EHD force acts on the gas predominantly downstream, with a transverse component towards the wall. The magnitude of the force depends on the shape of the electrode, Fig. 3a, which also affects the flow actuation, Fig. 3b. Numerical experiments [7] show that an optimum gap exists between the actuators kept at a phase difference for maximum force inducement, Fig. 3c, and for most effective separation mitigation, Fig. 3d. The effectiveness of flow control becomes limited for more than three actuators employed in phase, Fig. 3e-f. The effectiveness can be further increased if the actuators are at an optimum phase difference.

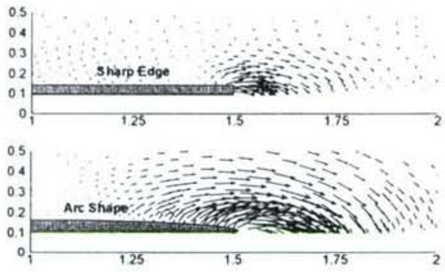

(a) EHD force distribution

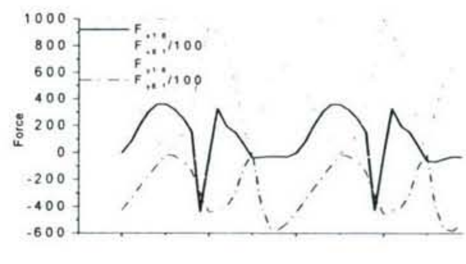

(c) Force components near electrodes at phase lag

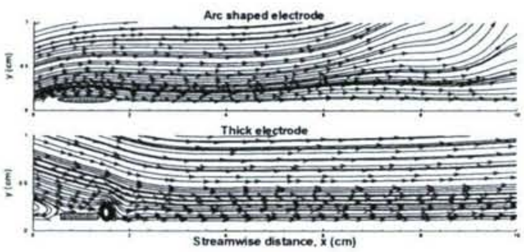

(b) Separation control

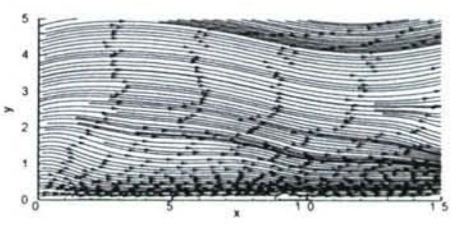

(d) Actuators (in red) at optimum phase lag and distance

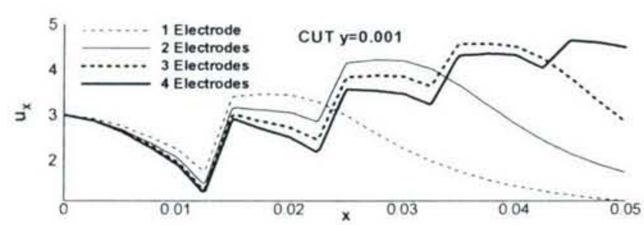

(e) Effect of electrodes on flow actuation 1 mm above wall

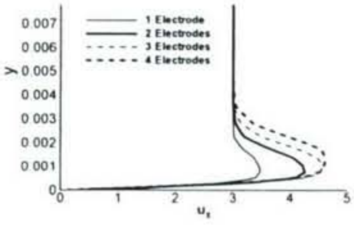

(f) Flow along vertical lines 4 mm downstream of the last actuator

Figure 3: Effects of various design parameters.

4. Air Chemistry: Earlier we have employed helium as working gas for its simplicity and stability of the discharge. In Fig. 4a-d surface discharge has been studied using air chemistry of formation of different ion and neutral species of nitrogen and oxygen about an asymmetric dielectric barrier plasma actuator. Species with very high recombination rates have been neglected for simplicity. Response of electrons to the electric field is very fast as compared to ions due to small mass and high mobility of electrons. Density profiles of different species are nearly opposite to each other at positive and negative peaks of the cycle. Density profiles of nitrogen atom N and oxygen atom O are similar because these do not move due to electric field. Density profiles of N_2^+ and O_2^+ are similar to each other at any specific time instance because they respond to electric field in a similar manner. There is, however, difference in level of ionization of different species due to difference in rate coefficients. Fig. 4c shows an accumulation of charge very close (20 times Debye length) to the wall which results in a forward moving force vector distribution in Fig. 4d. A detail air chemistry model with Poisson-Navier-Stokes equations is also under development for exploration of the effect of a plasma actuator operating in air using realistic geometry and electrode configurations.

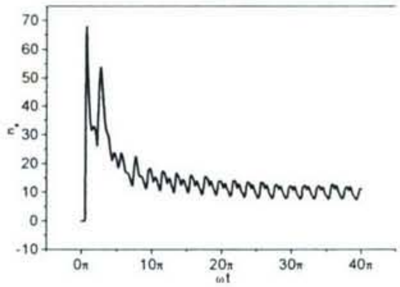

(a) Electron density reaches quasi-steady state.

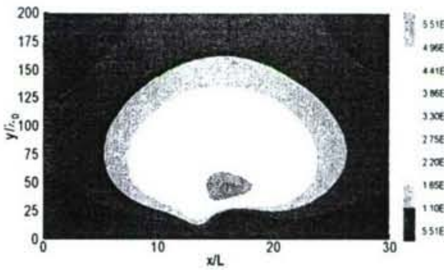

(b) Distribution of negative oxygen ion O^- at $\pi/2$.

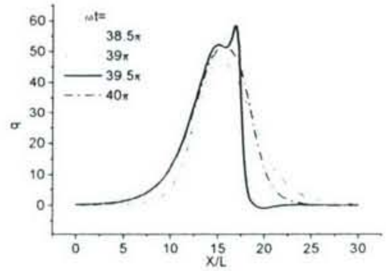

(c) Evolution of q = $e\,(o_2^+ + n_2^+ - n_e - o^-)$ at $20\lambda_D$

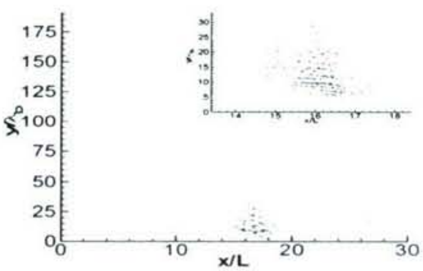

(d) Force vectors at the positive peak.

Figure 4: Solution details for surface barrier discharge using non-equilibrium air chemistry.

5. Integration of FDL3DI and MIG for Flow Control Simulation: Unsteady EHD force predictions from MIG have been successfully integrated into the FDL3DI fluid code in a collaborative effort with VAAC/AFRL researchers. Data integration system has been streamlined for smooth future transitions. Effective control of wing stall has been investigated for a 2 kV peak-to-peak voltage applied at 5kHz rf to an array of plasma actuators near the leading edge. Parameters varied include Reynolds number, angle of attack, duty cycle frequency and actuator strength and location. For details see Gaitonde et al. [9], and Visbal et al. [11]. Sample results plotted in Figs. 5a-c show that the three dimensional flow structure obtained with a force varying at radiofrequencies (5kHz) is significantly different in detail from that obtained with a steady actuator. By exciting instabilities in the separated shear layer, fine scale features arise through transition to turbulence, which are absent in steady actuation.

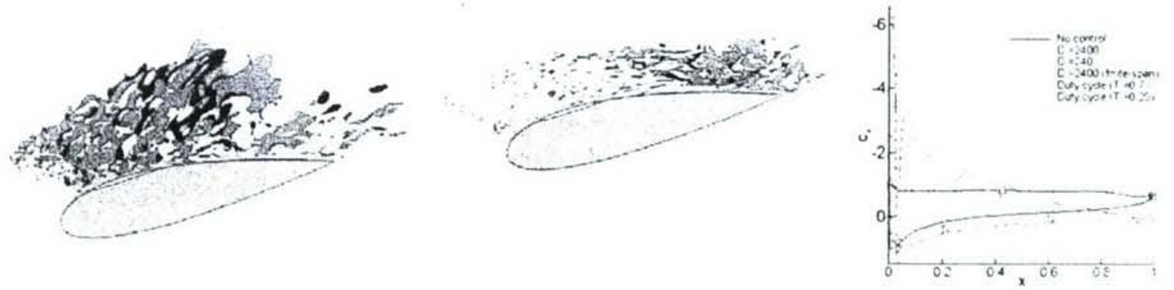

(a) (b) (c)

Figure 5: Unsteady control of wing stall at 15 deg AOA [9,11]. (a) Plasma actuators off. (b) Plasma actuators on. (c) Mid-span pressure coefficients at various plasma strengths.

Future Work

The developed model is now being employed for evaluating the flow control effect over a vehicle forebody using a polyphase power supply for various waveforms and duty cycles. The code is being extended to more complex air chemistries relevant for non-equilibrium, non-thermal plasma with asymmetric dielectric coated electrode configuration.

Acknowledgment/Disclaimer

This work was sponsored by the Air Force Office of Scientific Research, USAF, under grant number FA9550-05-1-0074. The views and conclusions contained herein are those of the authors and should not be interpreted as necessarily representing the official policies or endorsements, either expressed or implied, of the Air Force Office of Scientific Research or the U.S. Government.

Personnel Supported During Duration of Grant

Richard Anderson	Graduate Student, Kettering University, Michigan
Haribalan Kumar	Graduate Student, Kettering University, Michigan
Kunwar P. Singh	Postdoc, Kettering University, Michigan
Subrata Roy	Associate Professor, Kettering University, Michigan

Relevant Publications

"Dielectric Barrier Plasma Dynamics for Active Control of Separated Flows," S. Roy, K.P. Singh and D. Gaitonde, Applied Physics Letters, 88 (12) 121501, 2006.

"Force interaction of high pressure glow discharge with fluid flow for active separation control," S. Roy and D. Gaitonde, Physics of Plasmas, 13 (2) 023503, 2006.

"Phase Effect on Flow Control for Dielectric Barrier Plasma Actuators," K.P. Singh and S. Roy, Applied Physics Letters, 89 (1) 011501, 2006.

"Three-dimensional plasma-based stall control simulations with couple first-principles approaches," D. Gaitonde, M. Visbal, and S. Roy, Keynote Lecture FEDSM2006-98553, ASME Joint U.S. - European Fluids Engineering Summer Meeting, Miami, 2006.

"Control of transitional and turbulent flows using plasma-based actuators," M. Visbal, D. Gaitonde and S. Roy, AIAA-2006-3230, AIAA Fluid Dynamics and Flow Control Conference, June 2006.

"Modeling of dielectric barrier discharge plasma actuator with atmospheric air chemistry," K.P. Singh, S. Roy and D. Gaitonde, AIAA-2006-3381, AIAA Fluid Dynamics and Flow Control Conference, 2006.

"Effective discharge dynamics for plasma actuators," S. Roy, K.P. Singh, H. Kumar, D. Gaitonde and M. Visbal, AIAA-2006-374, 44th Aerospace Sciences Meetings, Reno, NV, 2006.

"A coupled approach for plasma-based flow control simulations of wing sections," D. Gaitonde, M. Visbal and S. Roy, AIAA-2006-1205, 44th Aerospace Sciences Meetings, Reno, NV, 2006.

"Preliminary experiments of barrier discharge plasma actuators using dry and humid air," R. Anderson and S. Roy, AIAA-2006-0369, 44th Aerospace Sciences Meetings and Exhibits, Reno, NV, 2006.

"Flow actuation using radio frequency in partially-ionized collisional plasmas," S. Roy, Applied Physics Letters, 86 (10) 101502, 2005.

"Multidimensional hydrodynamic plasma-wall model for collisional plasma discharges with and without magnetic field effects," H. Kumar and S. Roy, Physics of Plasmas, 12 (9) 093508, 2005.

"Simulation of an asymmetric single dielectric barrier plasma actuator," K.P. Singh and S. Roy, Journal of Applied Physics, 98 (8) 083303, 2005.

"Modeling of ionized gas flow about an asymmetric single dielectric barrier plasma actuator," S. Roy, FEDSM2005-77492, Plenary Lecture, ASME Fluids Engineering Division Summer Conference, 2005.

"Multidimensional collisional dielectric barrier discharge for flow separation control at atmospheric pressures," S. Roy and D. Gaitonde, AIAA-2005-4631, June 2005.

"Control of flow past a wing section with plasma-based body forces," D. Gaitonde, M. Visbal and S. Roy, AIAA-2005-5302, 36th AIAA Plasma Dynamics and Lasers Conference, Toronto, Canada, June 2005.

"Modeling Surface Discharge Effects of Atmospheric RF on Gas Flow Control," S. Roy and D. Gaitonde, AIAA-2005-0160, 43rd Aerospace Sciences Meeting and Exhibit, 10-13 January, 2005.

Transitions

MIG code has been successfully coupled with FDL3DI code of VAAC/AFRL. MIG results for unsteady EHD force have been incorporated in to the VAAC finite difference numerical code for simulation of flow control over NACA airfoil. Results were reported in Gaitonde et al. AIAA-2005-5302, AIAA-2006-1205 and FEDSM2006-98553, and in Visbal et al. AIAA-2006-3230. Efforts are underway for first principle simulation of vortical flow control about low sweep delta wing. AFRL Contacts for these transitions are Drs. Datta Gaitonde (937-904-4031) and Miguel Visbal (937-255-2551).

Patents

Electric Propulsion Device for High Power Applications, (2005).

Honors & Awards Received

Fellow, ASME.

Associate Fellow, AIAA. Technical Chair, 36th AIAA Thermophysics Conference, June 2003.

Fellow, World Innovation Foundation.

Associate Editor, ASME Journal of Fluids Engineering.

Guest Editor, Special Section on Numerical Developments in CFD, Journal of Fluids Engineering, Vol. 127, Issue 4, 2005.

Plenary Lecture, "Modeling of Ionized Gas Flow About an Asymmetric Single Dielectric Barrier Plasma Actuator," ASME Fluids Engineering Conference, June 2005.

Member, Thermophysics Technical Committee, Electric Propulsion Technical Committee, AIAA.

Member, CFD Technical Committee, Fluid Mechanics Technical Committee, ASME.

AFRL Point of Contact

Datta Gaitonde, AFRL/VAAC, WPAFB, OH, Phone 937-904-4031.

References

1. Roth, J.R., Phys. Plasmas, **10**, 2117 (2003).
2. Corke, T. and Post, M., AIAA Paper No. 2005-0563.
3. Shalaev, V., Fedorov, A., Malmuth, N., et al., AIAA Paper No. 2003-0034.
4. S. Roy, Applied Physics Letters, **86** (10), 101502 (2005).

5. S. Roy, K.P. Singh and D. Gaitonde, Applied Physics Letters, **88** (12) 121501 (2006).
6. S. Roy and D. Gaitonde, Physics of Plasmas, **13** (2) 023503 (2006).
7. K.P. Singh and S. Roy, Applied Physics Letters, **89** (1) 011501 (2006).
8. K.P. Singh, S. Roy and D. Gaitonde, AIAA-2006-3381, 2006.
9. D. Gaitonde, M. Visbal, and S. Roy, Keynote Lecture FEDSM2006-98553, Miami, 2006.
10. I. A. Kossyi, A. Yu Kostinsky, A.A. Matveyev, et al., Plasma Sources Sci. Techol., **1**, 207 (1992).
11. M. Visbal, D. Gaitonde and S. Roy, AIAA-2006-3230, 2006.
12. D. Balagangadhar and S. Roy, Comput. Methods Appl. Mech. Engrg., 190, 5465 (2001).
13. S. Roy, B.P. Pandey, J. Poggie and D. Gaitonde, Physics of Plasmas, 10, 2578 (2003).